IEEE Access
Multidisciplinary ⋮ Rapid Review ⋮ Open Access Journal

Received 14 November 2023, accepted 23 November 2023, date of publication 27 November 2023, date of current version 1 December 2023.

Digital Object Identifier 10.1109/ACCESS.2023.3336990

RESEARCH ARTICLE

Enhancement-Mode HEMT Performance and Mitigating Delay Through Double-Heterojunction With Connect Channel Utilization for Trap Effect Reduction

LONGFEI YANG[1], HUIQING SUN[1], RUIPENG LV[1], ZHEN LIU[1], YUANHAO ZHANG[1], PENGLIN WANG[1], YUAN LI[1], YONG HUANG[2], AND ZHIYOU GUO[1]
[1]Institute of Semiconductors Science and Technology, South China Normal University, Guangzhou 510006, China
[2]Guangdong Polytechnic Normal University, Guangzhou 510665, China

Corresponding author: Huiqing Sun (sunhq@scnu.edu.cn)

This work was supported in part by the Key-Area Research and Development Program of Guangdong Province under Grant 2020B010171002 and Grant 2019B010128002, and in part by the Guangdong Province Basic and Applied Technology Research Fund Project under Grant 2022A1515010127.

ABSTRACT This paper presents a GaN-based High Electron Mobility Transistor (HEMT) with a connected dual-channel structure (CDC-HEMT). Specifically, the $Al_{0.05}Ga_{0.95}N$ layer beneath the first channel enables the second channel to be in a non-conducting state while simultaneously increasing the number of electrons available in the conducting state. In contrast to conventional normally-off devices, the CDC-HEMT exhibits excellent DC performance, with a saturation current density increase from 0.67 A/mm to 1.52 A/mm at V_{ds} = 10 V and a maximum transconductance increase from 0.30 S to 0.62 S, which is twice as much. Furthermore, the optimal transconductance interval is widened by 1 V. The RF performance of the devices also demonstrates remarkable performance, with a current gain cut-off frequency of 31.8 GHz and a maximum oscillation frequency of 77 GHz. Under square wave testing, the transistors exhibit extremely low delay. The exceptional findings showcased in this study provide compelling evidence that the CDC-HEMT structure is a highly promising technique for utilizing GaN-based HEMTs with superior performance in power switching and microwave applications.

INDEX TERMS Connect-dual-channel, double heterojunction, GaN normally-off HEMT, trap offset, P-GaN gate.

I. INTRODUCTION

Gallium Nitride (GaN) is a well-established material system with wide-ranging applications in power switching and microwave technology. Its remarkable properties, such as a wide bandgap, high breakdown voltage, and exceptional electron mobility, have made it a material of choice for various technological applications [1], [2], [3], [4]. The AlGaN/GaN heterojunction, in particular, exhibits piezoelectric and spontaneous polarization effects, leading to a significantly elevated two-dimensional electron gas (2DEG) density, which further enhances its suitability for diverse applications.

Conventional HEMTs are typically normally-on devices, which can pose challenges in practical applications. These devices require a negative voltage power supply to turn them off, introducing the risk of unintended activation in the circuit. To address this issue, normally-off HEMTs have been developed. These devices remain non-conductive at zero bias, eliminating the need for a negative voltage power supply during non-operational states. This approach not only reduces power loss in the circuit but also simplifies overall circuit design, all while preserving the device's RF capabilities [5]. Recent advancements in GaN-on-Si(111)

The associate editor coordinating the review of this manuscript and approving it for publication was Rocco Giofrè.

© 2023 The Authors. This work is licensed under a Creative Commons Attribution-NonCommercial-NoDerivatives 4.0 License.
For more information, see https://creativecommons.org/licenses/by-nc-nd/4.0/

MOSHEMT technology have showcased its potential for advanced RF applications, with a record-breaking fmax of 700 GHz, highlighting its integration with Si CMOS [6].

Various methods have been explored to realize normally-off devices, including the use of P-GaN caps [7], [8], [9], [10], recessed gates [11], [12], [13], fluorine ion injection [14], [15], and cascode structures [16]. However, enhanced HEMTs often suffer from significant parasitic capacitance, adversely affecting their frequency characteristics [17]. Additionally, their low saturation current limits their utility in RF applications, hampering their widespread adoption. These limitations are partly attributed to traps present in the buffer layer [18], [19], [20].

While the literature on GaN HEMTs has primarily focused on traditional AlGaN/GaN single-heterostructure HEMTs, double-channel HEMTs have gained attention due to their potential for high current drive, rapid frequency response, and lower barrier carrier channels without experiencing current collapse [21]. Researchers like R. Mohapatra et al. [22] have made significant advancements by enhancing transconductance and DC characteristics through the utilization of a double-channel structure, offering innovative solutions for HEMTs. Wenjie Song et al. [23] have significantly improved the RF characteristics of HEMTs by employing a double-heterostructure with a T-gate structure.

In this paper, we introduce a novel approach, combining AlGaN/GaN double-channel HEMTs with P-GaN, to achieve a HEMT with favorable DC and RF characteristics while also realizing normally-off functionality. Conventional normally-off devices often suffer from drawbacks such as small opening current, low transconductance, and low operating frequency. Our focus is on harnessing the potential of the connected dual-channel structure to overcome these limitations and achieve normally-off HEMTs. To evaluate the performance and characteristics of the proposed device, we conducted Technology Computer Aided Design (TCAD) simulations.

II. DEVICE STRUCTURE AND PHYSICAL MODEL

The proposed GaN epitaxial structure consists of two 35 nm UID-GaN channel layers, two $25-\mathrm{nm}Al_{0.23}Ga_{0.77}$ N barrier layers, a concentration of 3×10^{17} cm^{-3} of P – GaN under the gate, and an $Al_{0.05}Ga_{0.95}$ N composition as a connect channel and buffer as shown in Fig.1(a). The lower channel and barrier under the gate-source edge have an $Al_{0.05}Ga_{0.95}$ N composition as a connect channel and a length of 100 – nm, which is represented in Fig.1(a) by the term "connect". The gate length (L_G), source to gate distance (L_{SG}), and gate to drain distance (L_{GD}) are 0.3 (Utilizing a commonly used gate length dimension for RF applications), 1, and 2.5μm, respectively (see Table 1).To ensure a realistic reflection of real-world conditions, we have introduced some traps during the simulation process. Both upper and lower channel layers have been furnished with identical donor and acceptor traps. The donor traps have a density of 1.27×10^{18} cm^{-3} and their energy levels are situated 3.2eV above the valence band. The acceptor traps have a density of 7×10^{17} cm^{-3}, with energy levels positioned 0.36eV below the conduction band.

TABLE 1. Key parameters for the simulation.

symbol	Description	value
L_{gate}	Length of the gate	0.3μm
$T_{channel}$	GaN channel thickness	35nm
T_{cap}	P-GaN cap layer thickness	110nm
L_{gd}	Length of the gate and drain	2.5μm
L_{gs}	Length of the gate and source	1μm
$T_{barrier}$	$Al_{0.23}Ga_{0.77}N$ barrier layer thickness	25nm

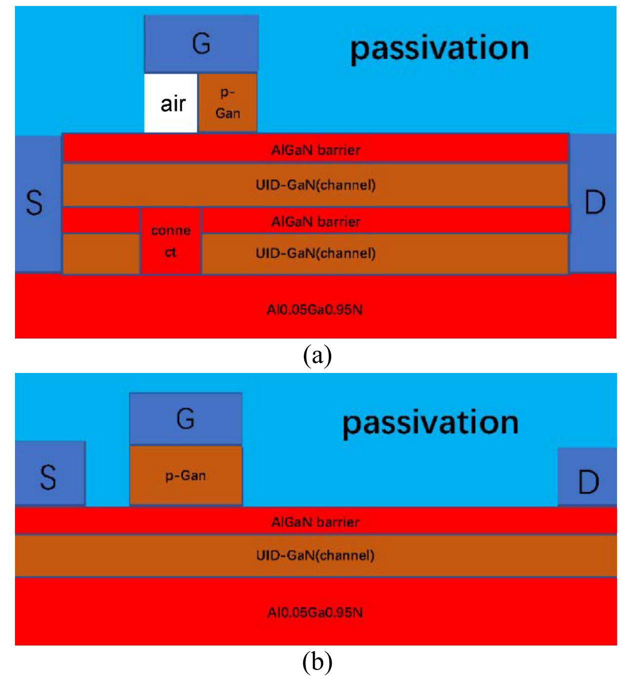

FIGURE 1. (a) Structure of normally-off GaN-based HEMT with CDC structure. (b) Conventional structure.

The purpose of the P-GaN cap layer is to deplete the upper channel and allow the gate to control the device. An air gap is introduced to reduce unwanted capacitance. The connected dual-channel (CDC) structure is added to deplete the local 2DEG in lower channel and make it non-conductive under $V_{ds} = 0$ V. The conventional structure is shown in Fig. 1. (b).

To improve the accuracy of the simulation, TCAD was utilized with several models. Specifically, the Fermi-Dirac distribution model was used to simulate degenerate semiconductor, while the SRH(Shockley-Read-Hall) concentration-dependent lifetime model was employed to account for the concentration-dependent carrier generation and recombination effects in the GaN channel. In addition, the PCH.INS model was utilized to include polarization charges along interfaces with insulators or the outside domain. The GANSAT.N model was also employed to describe the GaN high field mobility based on a fit to Monte Carlo data for nitride materials. Through these models, the simulation was

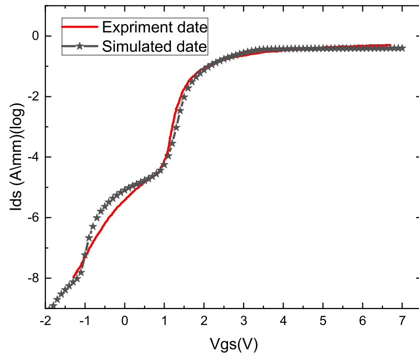

FIGURE 2. Measured and simulated I-V characteristics for a conventional HEMT with Lds = 10.4μm in logarithmic coordinates [24].

TABLE 2. Material property used in silvaco atlas TCAD.

SYMBOL	ALGAN	GAN
ENERGY BAND GAP(EV)	4.9	3.5
ELECTRON AFFINITY	3.41	4.0
PERMITTIVITY E(10^{18}/CM^3)	8.8	8.9
CONDUCTION BAND STATE DENSITY(10^{18}/CM^3)	2.71	2.23
VALANCE BAND STATE DENSITY(10^{18}/CM^3)	2.06	2.51
ELECTRON SATURATION VELOCITY(10^7/S)	1.1	2.5
ELECTRON MOBILITY(CM^2/VS)	300	1200

able to accurately simulate the behavior of the proposed GaN HEMT device. Table 2 presents the intrinsic material properties that were incorporated into the ATLAS TCAD simulation.These properties reflect the fundamental characteristics of the materials employed in the simulation and are vital for ensuring an accurate representation of the device's behavior.

The measured transfer characteristics, as depicted in Fig. 2, exhibit a close agreement between the simulated and experimental results. This strong correlation demonstrates the validity and accuracy of the proposed model. It should be noted that this study is primarily based on simulation work and does not directly involve measurements on actual devices. Furthermore, we acknowledge that there are notable differences in dimensions between the devices fabricated by Hilt et al. and the focus of our research. This difference arises because our work is grounded in theoretical modeling and simulations. Therefore, in terms of comparisons, we will ensure that they are conducted under the same physical conditions to effectively assess performance differences among various devices

III. RESULT AND DISCUSSION

A. ANALYSIS OF DC PERFORMANCE

We performed DC analysis to extract the transconductance and ID-VD families of curves, which are indicative of the gate of the device controllability and linearity. The transfer characteristics of the GaN HEMT at a bias voltage of 10V are shown in Fig.3.

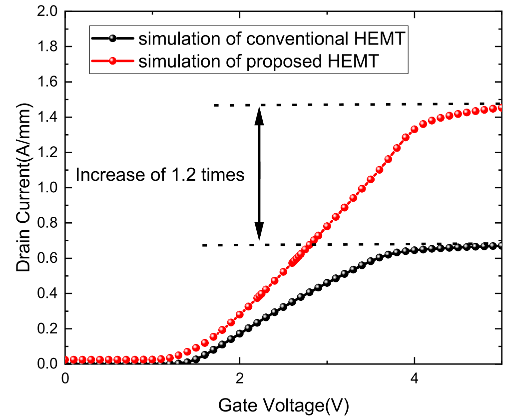

(a)

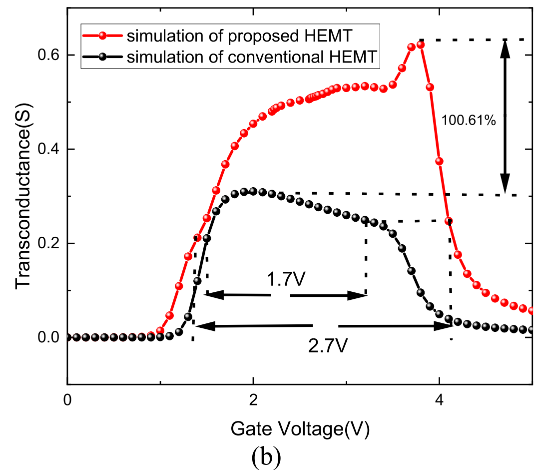

(b)

FIGURE 3. (a) Transfer characteristics and (b) transconductance (g_m) characteristics of AlGaN/GaN HEMT at V_{ds} = 10V.

The proposed device with the new P-GaN Cap with CDC structure was simulated, and the resulting drain current was 1.45A/mm, which is significantly higher compared to the traditional structure in the same simulation environment. The connect-dual-channel structure has greatly enhanced the current density, resulting in 1.2 times increase and a stronger device capability. Additionally, the maximum transconductance has doubled and the best width of transconductance has increased by 1V.

As shown in Fig.4, by means of the Ids-Vds measurement, it demonstrates that the CDC structure significantly enhances the DC characteristics.

B. RF PERFORMANCE

For millimeter-wave applications, the current gain is a critical parameter because it determines the unity current gain cut-off frequency (f_t). Therefore, small-signal simulation of the AlGaN/GaN HEMT with CDC structure was performed in ATLAS to extract and analyze the cut-off frequency (f_{max}), as shown in Fig.5.

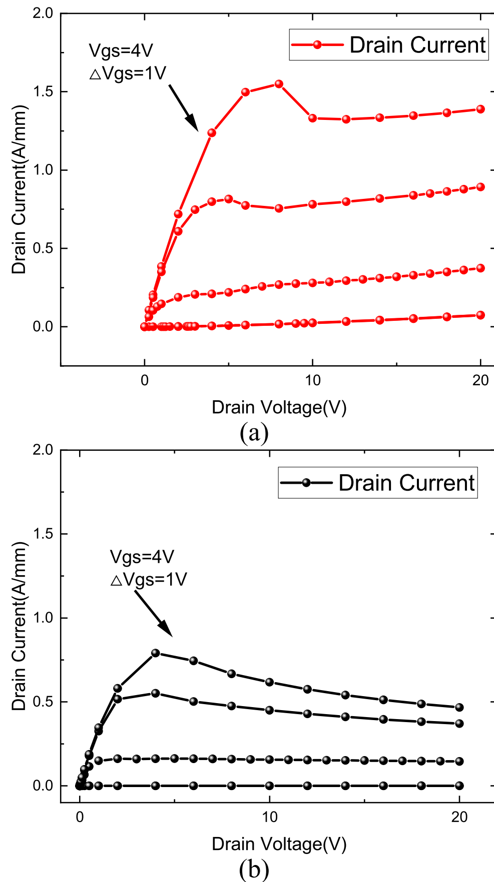

FIGURE 4. ID-VD Families of curves. (a). Proposed HEMT and (b). Conventional HEMT.

The proposed CDC-HEMT shows significant improvement in both current gain cut-off frequency (f_t) and unilateral power gain frequency (f_{max}) compared to the conventional HEMT. The f_t value increased from 26.3 GHz to 31.8 GHz, f_{max} value increased from 53.9 GHz to 77 GHz, while the f_{max} value increased by 20.9% and 42.8% for the proposed HEMT, respectively. The increase in transconductance and reduction in buffer-traps contribute to the improvement in frequency performance.

C. TRANSIENT RESPONSE

Fig.6(a) illustrates the initial biasing of the device with a gate voltage of 0 volt and a drain voltage of 5 volts. After 10 nanoseconds under this bias, the device undergoes a field-stressing phase for an additional 30 nanoseconds. During this field-stressing period, the drain voltage is raised to 25 volts, while the gate voltage is adjusted to 3 volts. Following this brief period of biased stress, the device is restored to its original biasing state, where in the gate voltage remains at 0 volts and the drain voltage at 5 volts. After only one millisecond of such biased stress, a significant reduction in the drain current is observed, thereby indicating the presence of the current collapse phenomenon. The definition of "delay" refers to the time it takes for the current to recover from its lowest point to a near-steady state after applying

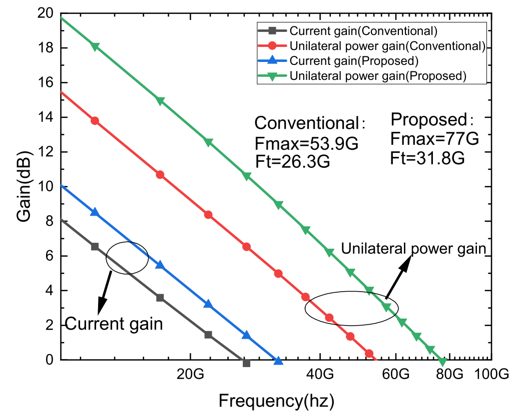

FIGURE 5. Current gain and unilateral power gain versus frequency under V_{ds} = 10V and V_g = 3V.

a voltage pulse. The conventional device exhibits strong current collapse effect, almost 100%, as shown in Fig.6(b), at the same time, the turn-on delay reached 1350 ps, while the turn-off delay was 300 ps. This effect seriously affects the normal use of the device under high-frequency signals. Although the HEMT with the new structure also exhibits serious current collapse, it can still be used normally. At the same time, it has an extremely low delay, as shown in Fig.6(c) at the same time, the turn-on delay reached 1150 ps, while the turn-off delay was 112 ps. It can be observed from Fig.6(c) that the proposed HEMT has better transient characteristics and output current swing, and has a faster recovery time from current collapse. These results illustrate that the dual-channel structure offsets traps and provides electrons.

IV. PHYSICAL INSIGHT

Fig.7 presents a comparison of the conductive band energy and electron concentration with and without the CDC structure in the proposed GaN HEMT where the position is as shown in Fig.7(a). The energy band diagrams illustrate the energy levels of electrons within the device and provide valuable insights into its performance.Fig.7(b) can be seen that the CDC structure elevates the local energy band, so that it can effectively prevent the second channel from conducting in the case of no bias, which is key for the device to become normally-off device. Fig.7 (c) shows the energy band and electron concentration of a common double heterojunction without CDC structured HEMT. The second channel has 2DEG, which is not controlled by the gate, due to the second barrier layer pulling down the energy band diagram, making the device not work properly at $V_{gs} = 0$. Fig.7(d) shows the band diagram and electron concentration in the conducting state of an HEMT with CDC structure. It can be seen that in the connection layer, after the gate and source-drain voltage rise, the 2DEG originally depleted due to the presence of the connection layer begins to form again and becomes involved in conducting electricity. In summary, Fig.8 provides essential visual evidence of how the CDC structure positively influences the device's band diagram and enhances

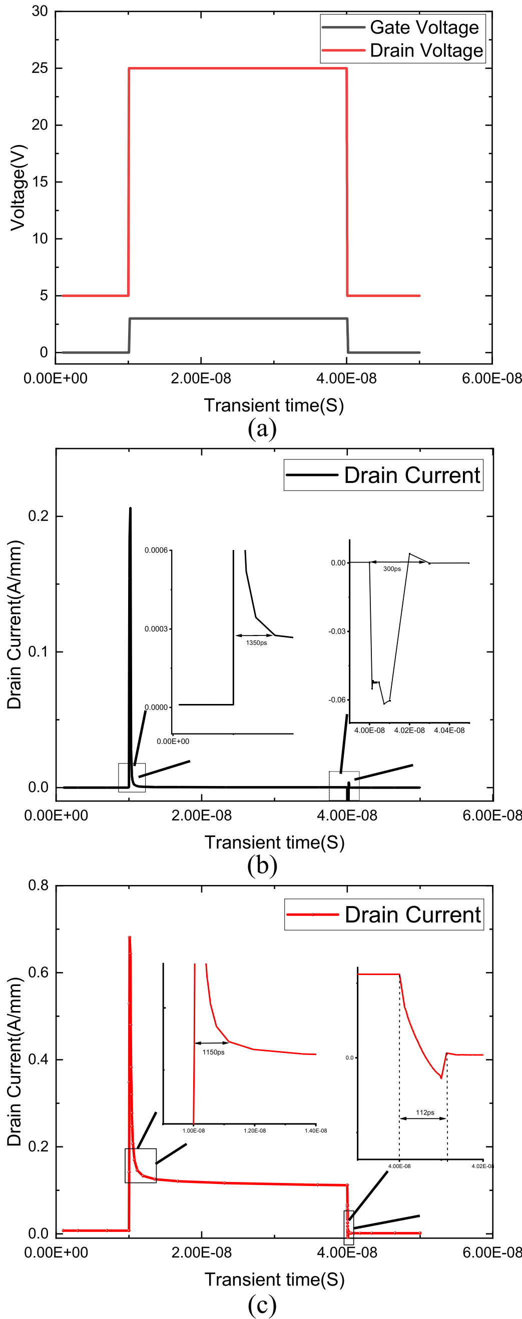

FIGURE 6. **Transient response (a).test signal (b). conventional HEMT. (c). Proposed HEMT.**

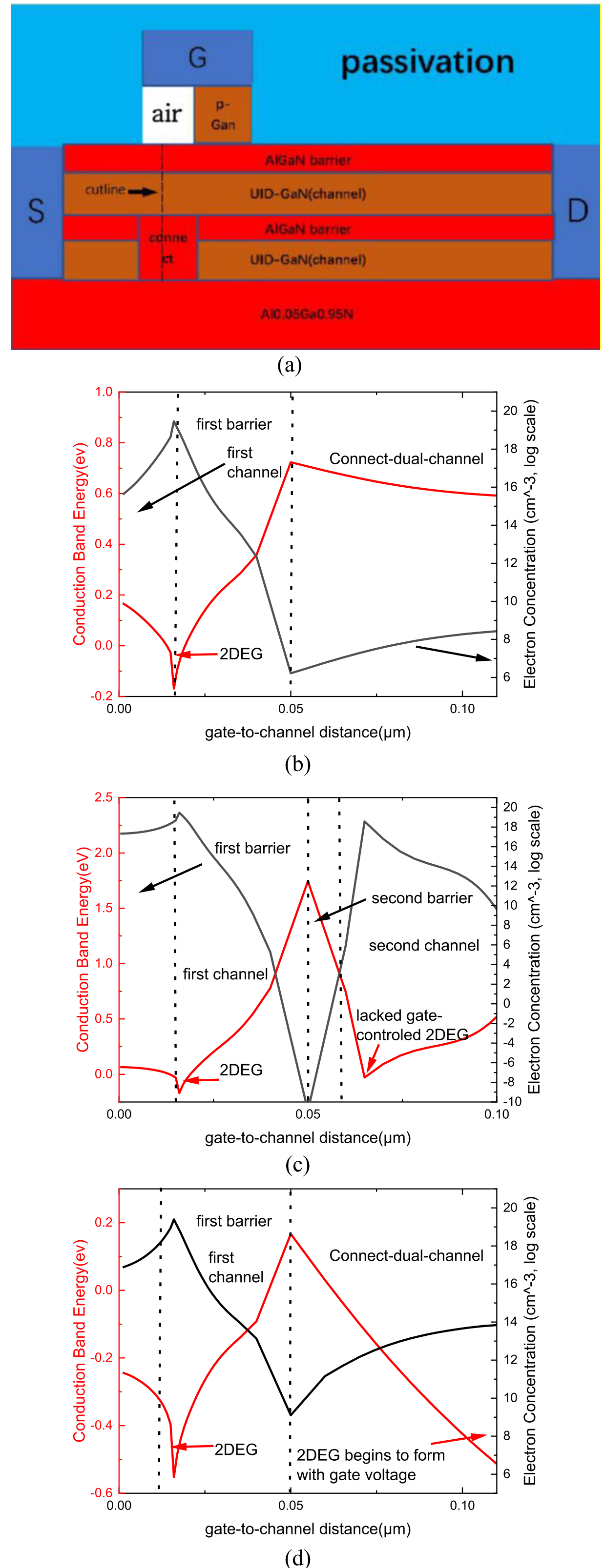

FIGURE 7. **(a). Schematic of the Proposed HEMT with Noted Cutline. (b) Conduction band energy and electron concentration with connected channel (from top to bottom of the cutline). (c) Conduction band energy and electron concentration without connected channel (from top to bottom of the cutline). (d) Conduction band energy and electron concentration with connected channel in the on state (from top to bottom of the cutline).**

its performance by achieving enhancement-mode functionality and enabling gate control of both heterostructures. This validates the effectiveness of the proposed CDC structure in the GaN HEMT design.

One reason for the increase in current and transconductance is the participation of the second channel in conduction during the on-state, as described in the band diagram above. The participation of the second channel in conduction during the on-state, due to the presence of coupling effects between the two channels. Around 4V, these effects are maximized, leading to the greatest variation in current and

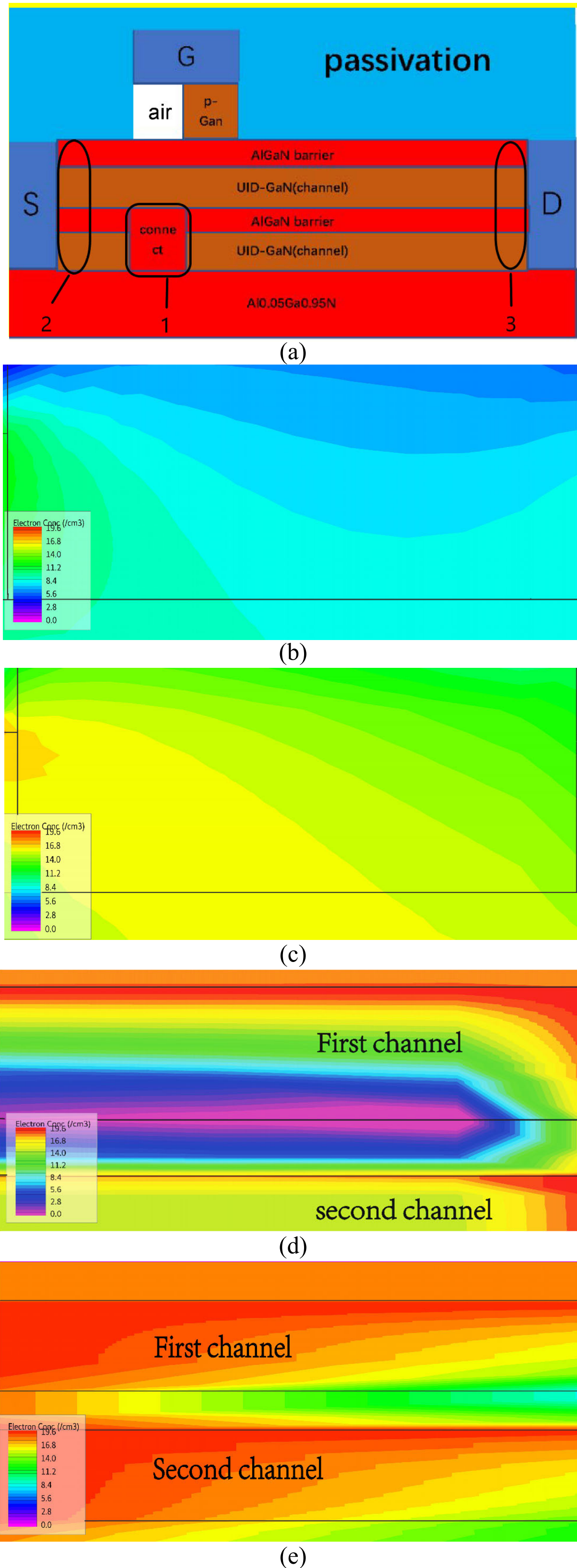

FIGURE 8. (a).Schematic of the Proposed HEMT with Noted Boxes(b).Electron Concentration in Connect Channel at Off-State (Noted Box 1).(c).Electron Concentration in Connect Channel at On-State (Noted Box 1).(d) Electron Concentration in Gate-to-Drain at On-State (Noted Box 2).(e).Electron Concentration in Gate-to-Source at Off-State (Noted Box 3).

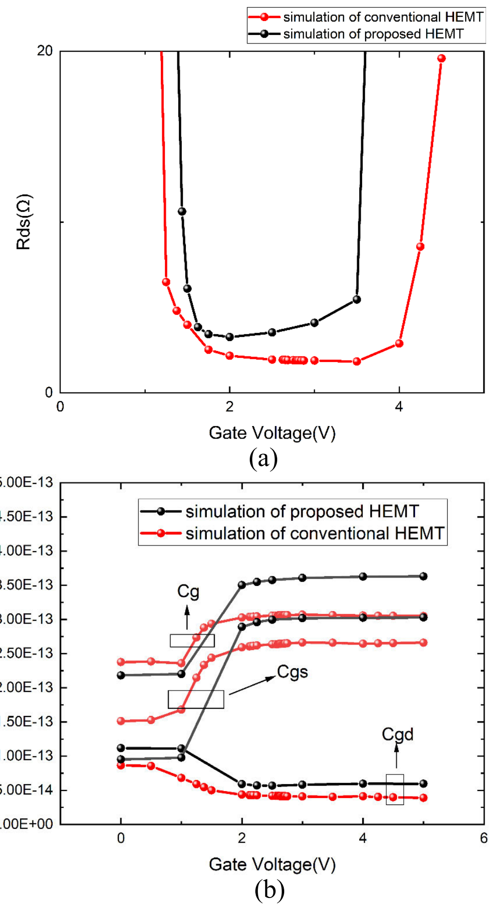

FIGURE 9. Parasitic Parameter (a) and Drain-Source Resistance (b) with Capacitance. (V_d = 10 V, Small-Signal Analysis, 3.6 GHz).

consequently resulting in the peak of transconductance. As shown in Fig. 8(b) and (c), the electron concentration in the connect channel differs by nearly seven orders of magnitude between on and off states. Fig. 8(d) and (e) indicate that the two channels are in parallel during the conducting state.

In summary, the CDC structure enables the gate to control two conductive channels simultaneously enhancing the gate's control effect. This enhancement is the main reason for the improvement in transconductance and current. According to the former reports, under short channel limit, the $I_{dsat}/f_t/f_{max}$ can be expressed as follows:

$$I_{DSAT} \approx \beta V_{ds}(V_G - R_{ds}I_{Dsat}) \tag{1}$$

$$f_T = \frac{g_m/2\pi}{[C_{gs}+C_{gd}]\cdot[1+(R_s+R_d)/R_{ds}]+C_{gd}\cdot g_m\cdot(R_S+R_D)} \tag{2}$$

$$f_{\max} \approx \frac{f_t}{2\sqrt{\frac{(R_i+R_s+R_g)}{R_{ds}}} + (2\pi f_t)R_G C_{gd}} \tag{3}$$

The parameter β is determined solely by the dimensions (length and width) of the device, and it indicates the device's intrinsic characteristics. On the other hand,

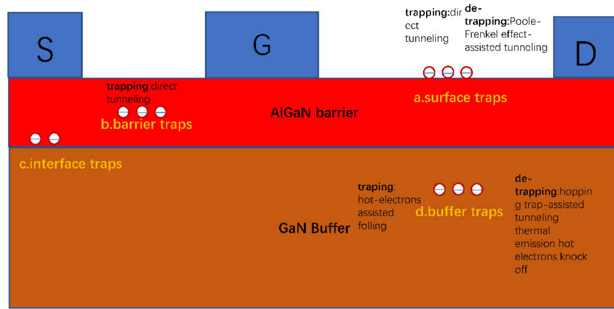

FIGURE 10. Main trapping behaviors in the GaN/AlGaN HEMT.

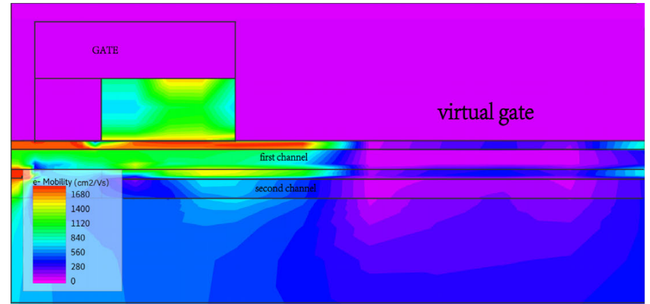

(a)

(b)

FIGURE 11. Virtual gate effect (a). Proposed HEMT. (b). Conventional HEMT.

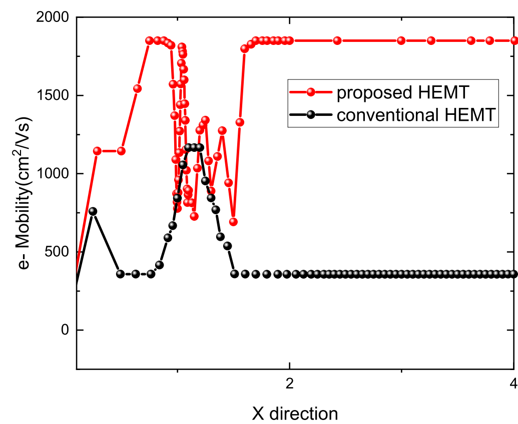

FIGURE 12. Electron mobility along the horizontal channel (source to drain axis).

g_m (transconductance) represents the ability of the device to convert input voltage variations into output current variations, while R_{ds} (drain-to-source resistance) represents the resistance experienced by the current flowing from the drain to the source. In addition, the capacitances C_{gd} (gate-to-drain capacitance) and C_{gs} (gate-to-source capacitance) represent the inherent capacitive coupling between the gate and the drain, and the gate and the source, respectively. These capacitances play a crucial role in determining the high-frequency performance and dynamic behavior of the device. Equation 1 indicates that an increase in current can be achieved by decreasing the drain-to-source resistance and enhancing the transconductance, as illustrated in Fig. 9(a). At the same time the effect of stray capacitance cannot be disregarded, as shown in Fig. 9(b). During the on-state operation at the 3.6 GHz test, When the gate voltage is below 2V, our newly proposed device exhibits relatively small capacitance levels, except for C_{gd}. However, as the gate voltage increases, the device's capacitance experiences significantly greater growth compared to traditional devices. Despite the increased capacitance at higher gate voltages in our novel device, its RF performance remains notably superior to that of conventional devices. This is primarily attributed to the compensatory effect of the dual-channel structure and enhanced gate control effect (improved g_m), especially in low-voltage conditions, where RF performance experiences significant enhancements. Regarding the substantial increase in capacitance as a consequence of increasing voltage in our novel device, I posit that it is primarily linked to charge accumulation. The dual-channel structure prompts the direct accumulation of electrons between the upper GaN layer and the lower AlGaN barrier, as visibly illustrated in Fig. 8(c) and (d). This electron accumulation phenomenon becomes progressively more pronounced at elevated voltages, particularly within the lower AlGaN barrier region. Here, it effectively serves as a back-barrier, severely impeding electron mobility and consequently resulting in amplified capacitance.

The improvement in transient characteristics is mainly due to faster electron velocity and a decrease in gate-lag. Gate-lag is mainly caused by acceptor-like traps in the AlGaN/GaN interface and buffer [25], [26], [27], which create a virtual-gate (as shown in Fig.10). The presence of the second barrier acts as a back barrier, preventing the hot-electron effect in the first channel, resulting in an increased electron velocity.

Fig.11 (a) shows the electron mobility and virtual gate effect of HEMTs with CDC structure in the gate nearby, and Fig.11 (b) shows the electron mobility without CDC structure, it can be seen that the CDC structure greatly weakens the virtual gate effect because the electrons in the secondary channel greatly compensate for the trap in the channel layer itself. On the other hand, the ability to conduct electricity has been promoted due to the double channel providing a large number of electrons. Fig.12 illustrates that the CDC structure significantly increases electron mobility within the channel.

As can be seen in Fig.5, despite the huge increase in current, the proposed device shows a significant kink effect compared with the conventional device. The main reason is that the deep-level traps in the GaN channel could trap and de-trap electrons. The mechanism of the kink effect is shown in Fig.13. If the energy level of the hot electron is

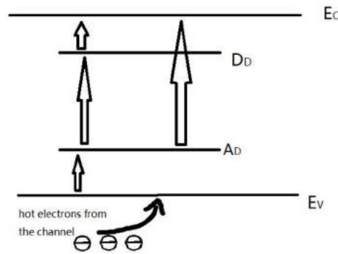

FIGURE 13. Mechanism of deep levels in Gan channel layer for kink effect.

raised high enough by a high source-drain voltage, valence band electrons are trapped in a deep-level trap and activated as acceptor-like, just as electrons move from Ev to A_D in Fig.13. The result is that the 2DEG reduces and the I_D-V_D curve decreases with drain voltage. With an increase in drain voltage, the electrons trapped by A_D will jump to D_D or E_c and be translated into electrons in the conductive band or donor-like traps in D_D. Then, the 2DEG increases and the I_D-V_D curve rises with drain voltage. Due to the accuracy requirement of double heterojunction simulation, a large number of deep-level defects are added to both channel layers, so the kink effect is inevitably enhanced in new devices.

V. CONCLUSION

The research presents a promising design for GaN HEMTs that has the potential to offer superior RF and DC performance with minimal switching loss and the physical mechanism is also analyzed. The CDC structure exhibited remarkable enhancements in terms of saturated current density, maximum transconductance, current gain cutoff frequency, and maximum oscillation frequency in comparison to traditional HEMTs. Moreover, the current collapse effect was well-managed, and the recovery time was faster, which further demonstrates the advantages of the proposed structure. This makes it a potential candidate for various industrial and research applications across a wide range of fields. The demonstrated performance and advantages of the CDC structure position it as a valuable option for advancing technological advancements in the realm of power and frequency-critical applications.

REFERENCES

[1] N. Islam, M. F. P. Mohamed, M. F. A. J. Khan, S. Falina, H. Kawarada, and M. Syamsul, "Reliability, applications and challenges of GaN HEMT technology for modern power devices: A review," *Crystals*, vol. 12, no. 11, p. 1581, Nov. 2022, doi: 10.3390/cryst12111581.

[2] J. Ajayan, D. Nirmal, P. Mohankumar, B. Mounika, S. Bhattacharya, S. Tayal, and A. S. A. Fletcher, "Challenges in material processing and reliability issues in AlGaN/GaN HEMTs on silicon wafers for future RF power electronics & switching applications: A critical review," *Mater. Sci. Semiconductor Process.*, vol. 151, Nov. 2022, Art. no. 106982, doi: 10.1016/j.mssp.2022.106982.

[3] K. Husna Hamza and D. Nirmal, "A review of GaN HEMT broadband power amplifiers," *AEU Int. J. Electron. Commun.*, vol. 116, Mar. 2020, Art. no. 153040, doi: 10.1016/j.aeue.2019.153040.

[4] M. A. K. Khan, M. A. Alim, and C. Gaquiere, "2DEG transport properties over temperature for AlGaN/GaN HEMT and AlGaN/InGaN/GaN pHEMT," *Microelectronic Eng.*, vol. 238, Feb. 2021, Art. no. 111508, doi: 10.1016/j.mee.2021.111508.

[5] A. Udabe, I. Baraia-Etxaburu, and D. G. Diez, "Gallium nitride power devices: A state of the art review," *IEEE Access*, vol. 11, pp. 48628–48650, 2023, doi: 10.1109/ACCESS.2023.3277200.

[6] H. W. Then, "Enhancement-mode 300-mm GaN-on-Si(111) with integrated Si CMOS for future mm-wave RF applications," *IEEE Microw. Wireless Technol. Lett.*, vol. 33, no. 6, pp. 835–838, Jun. 2023, doi: 10.1109/LMWT.2023.3268184.

[7] I. Hwang, J. Oh, H. S. Choi, J. Kim, H. Choi, J. Kim, S. Chong, J. Shin, and U.-I. Chung, "Source-connected p-GaN gate HEMTs for increased threshold voltage," *IEEE Electron Device Lett.*, vol. 34, no. 5, pp. 605–607, May 2013, doi: 10.1109/LED.2013.2249038.

[8] Y. Wu, S. Liu, J. Zhang, S. Zhao, X. Li, K. Zhang, Y. Ai, W. Zhang, T. Chen, and Y. Hao, "Novel in-situ AlN/p-GaN gate HEMTs with threshold voltage of 3.9 V and maximum applicable gate voltage of 12.1 V," *IEEE Trans. Electron Devices*, vol. 70, no. 2, pp. 424–428, Feb. 2023, doi: 10.1109/TED.2022.3228495.

[9] Y. Shi, Z. He, Y. Huang, Z. Cai, Y. Chen, L. Cheng, W. Chen, R. Sun, C. Liu, G. Lu, and B. Zhang, "A comparative study on G-to-S ESD robustness of the ohmic-gate and Schottky-gate p-GaN HEMTs," *IEEE Trans. Electron Devices*, vol. 70, no. 5, pp. 2229–2234, May 2023, doi: 10.1109/TED.2023.3257282.

[10] C. Zhang, S. Li, S. Liu, W. Lu, Y. Ma, J. Wei, L. Zhang, W. Sun, D. Wang, J. Zhou, and S. Bai, "Hybrid gate p-GaN power HEMTs technology for enhanced vth stability," in *IEDM Tech. Dig.*, San Francisco, CA, USA, Dec. 2022, p. 35, doi: 10.1109/IEDM45625.2022.10019437.

[11] D. R. Androse, S. Deb, S. K. Radhakrishnan, and E. Sekar, "T-gate ALGaN/GaN HEMT with effective recess engineering for enhancement mode operation," *Mater. Today, Proc.*, vol. 45, pp. 3556–3559, 2021, doi: 10.1016/j.matpr.2020.12.1076.

[12] H. Bhattacharjee, A. Dey, A. Saha, and P. Meher, "Threshold voltage analysis of E-mode recessed p-GaN gate HEMT—A simulation based study," in *Proc. IEEE Devices Integr. Circuit (DevIC)*, India, Kalyani, India, Apr. 2023, pp. 71–76, doi: 10.1109/DevIC57758.2023.10134842.

[13] T. Suemitsu, H. Yokoyama, Y. Umeda, T. Enoki, and Y. Ishii, "High-performance 0.1-μm gate enhancement-mode InAlAs/InGaAs HEMT's using two-step recessed gate technology," *IEEE Trans. Electron Devices*, vol. 46, no. 6, pp. 1074–1080, Jun. 1999, doi: 10.1109/16.766866.

[14] F. Shen, R. Hao, L. Song, F. Chen, G. Yu, X. Zhang, Y. Fan, F. Lin, Y. Cai, and B. Zhang, "Enhancement mode AlGaN/GaN HEMTs by fluorine ion thermal diffusion with high V_{th} stability," *Appl. Phys. Exp.*, vol. 12, no. 6, Jun. 2019, Art. no. 066501, doi: 10.7567/1882-0786/ab1cfa.

[15] C.-H. Wu, P.-C. Han, Q. H. Luc, C.-Y. Hsu, T.-E. Hsieh, H.-C. Wang, Y.-K. Lin, P.-C. Chang, Y.-C. Lin, and E. Y. Chang, "Normally-OFF GaN MIS-HEMT with F-doped gate insulator using standard ion implantation," *IEEE J. Electron Devices Soc.*, vol. 6, pp. 893–899, 2018, doi: 10.1109/JEDS.2018.2859769.

[16] V. Dj. Vukic, J. Mrvic, and V. A. Katic, "Comparison of the switching energy losses in cascode and enhancement-mode GaN HEMTs," in *Proc. 20th Int. Symp. Power Electron. (Ee)*, Novi Sad, Serbia, Oct. 2019, pp. 1–5, doi: 10.1109/PEE.2019.8923198.

[17] M. Haziq, S. Falina, A. A. Manaf, H. Kawarada, and M. Syamsul, "Challenges and opportunities for high-power and high-frequency AlGaN/GaN high-electron-mobility transistor (HEMT) applications: A review," *Micromachines*, vol. 13, no. 12, p. 2133, Dec. 2022, doi: 10.3390/mi13122133.

[18] R. Ye, X. Cai, C. Du, H. Liu, Y. Zhang, X. Duan, and J. Zhu, "An overview on analyses and suppression methods of trapping effects in AlGaN/GaN HEMTs," *IEEE Access*, vol. 10, pp. 21759–21773, 2022, doi: 10.1109/ACCESS.2021.3139443.

[19] A. Chakraborty and D. Biswas, "Comparison of trap characteristics between AlGaN/GaN and AlGaN/InGaN/GaN heterostructure by frequency dependent conductance measurement," *Appl. Phys. Lett.*, vol. 106, no. 8, Feb. 2015, Art. no. 082112.

[20] G. Longobardi and F. Udrea, "On the time-dependent transport mechanism between surface traps and the 2DEG in AlGaN/GaN devices," *IEEE Trans. Electron Devices*, vol. 64, no. 11, pp. 4415–4423, Nov. 2017, doi: 10.1109/TED.2017.2752859.

[21] R. Chu, Y. Zhou, J. Liu, D. Wang, K. J. Chen, and K. M. Lau, "AlGaN-GaN double-channel HEMTs," *IEEE Trans. Electron Devices*, vol. 52, no. 4, pp. 438–446, Apr. 2005.

[22] R. Mohapatra and P. Dutta, "Improvement of transconductance in double channel AlGaN/GaN HEMT," in *Proc. Int. Conf. Appl. Electromagn., Signal Process. Commun. (AESPC)*, vol. 1, Bhubaneswar, India, Oct. 2018, pp. 1–3, doi: 10.1109/AESPC44649.2018.9033336.

[23] W. Song, Z. Zheng, T. Chen, J. Wei, L. Yuan, and K. J. Chen, "RF linearity enhancement of GaN-on-Si HEMTs with a closely coupled double-channel structure," *IEEE Electron Device Lett.*, vol. 42, no. 8, pp. 1116–1119, Aug. 2021, doi: 10.1109/LED.2021.3087785.

[24] O. Hilt, A. Knauer, F. Brunner, and E. Bahat-Treidel, "Normally-off AlGaN/GaN HFET with p-type Ga Gate and AlGaN buffer," in *Proc. 6th Int. Conf. Integr. Power Electron. Syst. (CIPS)*. Nuremberg, Germany: ETG Fachbericht, 2010, pp. 185–188.

[25] A. Nakajima, K. Fujii, and K. Horio, "Numerical analysis of buffer-trap effects on gate lag in AlGaN/GaN high electron mobility transistors," *Jpn. J. Appl. Phys.*, vol. 50, no. 10R, Oct. 2011, Art. no. 104303.

[26] C. Miccoli, V. C. Martino, S. Reina, and S. Rinaudo, "Trapping and thermal effects analysis for AlGaN/GaN HEMTs by means of TCAD simulations," *IEEE Electron Device Lett.*, vol. 34, no. 9, pp. 1121–1123, Sep. 2013.

[27] M. Faqir, G. Verzellesi, A. Chini, F. Fantini, F. Danesin, G. Meneghesso, E. Zanoni, and C. Dua, "Mechanisms of RF current collapse in AlGaN-GaN high electron mobility transistors," *IEEE Trans. Device Mater. Rel.*, vol. 8, no. 2, pp. 240–247, Jun. 2008.

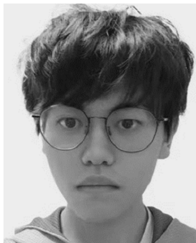

LONGFEI YANG received the M.S. degree from the Department of Applied Physics, Qingdao University of Science and Technology, China, in 2018. He is currently pursuing the M.A.Eng. degree in integrated circuit engineering with South China Normal University, China.

HUIQING SUN was born in Liaoning, China, in 1963. She was an Associate Professor with South China Normal University, China, in 2004. Her current research interest includes wide bandgap semiconductor materials and devices.

RUIPENG LV received the B.S. degree from the College of Electronic Information Engineering, Hebei University, China, in 2021. He is currently pursuing the M.S degree in optical engineering with South China Normal University, Guangzhou.

ZHEN LIU received the B.E. degree in information engineering from Huaqiao University, China, in 2022. He is currently pursuing the master's degree in microelectronics and solid-state electronics with South China Normal University, China.

YUANHAO ZHANG received the B.S. degree in electronic and information engineering from the China University of Mining and Technology, China, in 2022. He is currently pursuing the M.S. degree in new-generation electronic information technology with South China Normal University, China.

PENGLIN WANG received the B.S. degree from the Chengdu University of Electronic Science and Technology, China. He is currently pursuing the master's degree in electronics science and technology with South China Normal University, China.

YUAN LI received the B.S. degree in information display and photoelectric technology from the South China University of Technology, China, in 2016. He is currently pursuing the Ph.D. degree in electronics science and technology with South China Normal University, China.

YONG HUANG received the B.S. degree from Foshan University, in 2004, the M.S. degree from the South China University of Technology, in 2007, and the Ph.D. degree from South China Normal University, in 2018. His current research interests include GaN-based visible light communication LED and micro-LED.

ZHIYOU GUO was born in Liaoning, China, in 1959. He was a Professor with South China Normal University, China, in 2006. His current research interests include wide band gap semiconductor materials and devices and GaN-based micro LED devices for visible light communication.